*Desalination and Water Treatment*
www.deswater.com

doi: 10.5004/dwt.2021.27765

238 (2021) 117–124
October

# Optimization and modeling of the three-dimensional electrochemical process in the removal of ciprofloxacin from aqueous media with a central composite design

R. Shokoohi[a], M.R. Samarghandi[a], J. Faredmal[b], A. Moradi Behgoo[c,*]

[a]*Department of Environmental Health Engineering and Research Center for Health Sciences, School of Public Health, Hamadan University of Medical Sciences, Hamadan, Iran, emails: reza.shokohi@umsha.ac.ir (R. Shokoohi), Samarghandi@umsha.ac.ir (M.R. Samarghandi)*
[b]*Department of Statistics and Research Center for Health Sciences, School of Public Health, Hamadan University of Medical Sciences, Hamadan, Iran, email: javad.faradmal@umsha.ac.ir*
[c]*Environmental Health Engineering, School of Public Health, Hamadan University of Medical Sciences, Hamadan, Iran, Tel. +98 9183196114; email: amoradibehgoo@yahoo.com*

Received 1 October 2018; Accepted 20 August 2021

## ABSTRACT

Antibiotics cause many environmental problems due to bioaccumulation, drug resistance, and environmental stability. This study aimed to investigate the efficiency of a three-dimensional electrochemical process with aluminum electrodes (3D-ECPWAE) to remove ciprofloxacin from aqueous media. Furthermore, the effect of main operating parameters as independent variables (initial pH, pollutant concentration, current density, and electrolyte concentration) on ciprofloxacin (CIP) degradation efficiency as response variables was investigated and optimized by central composite design. The initial results were analyzed and optimized using Minitab 17. The confirmatory tests were performed at optimum conditions and the process efficiency to reduce CIP concentration, chemical oxygen demand (COD), and total organic carbon (TOC). These results indicate that under the optimum condition, the maximum CIP, COD, and TOC removal efficiency was 86.72%, 48.04%, and 45.45%, respectively. The optimal values of the variables for CIP concentration, pH, current intensity, and electrolyte concentration were 80 mg/L, 5.8, 0.75, and 0.4 g/L at the optimum time (30 min). According to the results, the acceptable efficiency of the 3D-ECPWAE for CIP removal was at a relatively high concentration at an appropriate time.

*Keywords:* Ciprofloxacin; Three-dimensional electrochemical; Response surface methodology; Total organic carbon; Central composite design

## 1. Introduction

Pharmaceuticals are a major source of water pollution due to inappropriate disposal in the water bodies by the pharmaceutical industries, inappropriate disposal of sewage sludge in soil, and human excretion [1]. The excessive and inappropriate use of antibiotics for human beings and livestock and the continuous introduction of environmental matrices lead to bioaccumulation in microorganisms. The high polarity and the non-volatile nature of antibiotics prevent them from getting out of environmental matrices [2]. Studies have shown that most sewage treatment plants can remove 60%–90% of the antibiotics [3]. The WHO has declared that the widespread application of antibiotics in aquacultures may cause risks for the consumer contributing to the antibacterial resistance in human and veterinary medicine due to the accumulation of their residues in edible tissues of fish. Ciprofloxacin

---

* Corresponding author.

1944-3994/1944-3986

(CIP) is an antibacterial agent and is a second-generation fluoroquinolone, widely used in human and veterinary medicine. It is also responsible for the destruction of both gram-negative and gram-positive bacteria through DNA inhibition, toxic to algae, and enhancing antibiotic-resistant bacteria's growth. It is also recalcitrant and resistant to biodegradation and releasing them into the environment can cause many adverse ecological effects including food destruction, cereal reproduction interactions, and nitrification process disruption [4–6]. The mean concentration of CIP is reported 150 μg/L in the hospital wastewater effluent, 0.6 μg/L in the municipal wastewater treatment plant influents and less than 1 μg/L in the surface waters [2]. Wastewater treatment using electrochemical methods received much attention during recent years. Electrochemical advanced oxidation processes are of great interest in decontaminating wastewaters polluted with toxic and persistent organic pollutants due to hydroxyl radicals in situ electrochemical production. The other advantages, such as versatility, high energy efficiency, amenability of automation, and cost-effectiveness, make electrochemical technologies an environment-friendly method. In particular, these techniques have the advantages of high efficiency, strong oxidation ability, simple equipment, operation under mild conditions, environmental compatibility, economic feasibility, and easy implementation ability [6]. Electrochemical oxidation is one such method used to treat wastewater, in which hydrogen peroxide and hydroxyl radicals are generated by electrolytic methods and used to degrade organic pollutants. Various electrochemical methods include anodic oxidation, electro Fenton, proxy coagulation, and electrocoagulation [7]. The 3D process is different from the 2D type due to the presence of a material called a third electrode. The third electrode is a particle electrode that contains granular material. This material lies inside the reactor between the two electrodes. By establishing an electric potential difference between the two electrodes, these particles are polarized and then form a large number of small charged electrodes. One of these charged particles serves as an anode, while the other serves as a cathode. In this case, with the particle microelectrodes, the 3D electrode process can have a higher efficiency than the 2D process [7,8]. The results of the comparison between the processes showed that the removal efficiency of CIP after 60 min of electrolysis time is reduced as follows: three-dimensional electro-Fenton (3DEF) > three-dimensional electrochemical (3DE) > electro-Fenton (EF) > two dimensional electrochemical (2DE) [9]. The chemical oxygen demand (COD) removal efficiency and $H_2O_2$ production in the 3DEF system were much higher than other electrocatalytic processes, which is related to the presence of MWCNTs-$Fe_3O_4$ as a particle electrode that can activate the molecular oxygen for higher production of hydrogen peroxide ($H_2O_2$) and hydroxyl radical ($^{\bullet}OH$). The MWCNTs-$Fe_3O_4$ nanocomposite indicated a high degree of stability and reusability [10]. In the three-dimensional electrochemical process, the type of particle electrode is one of the most important factors owing to its impact on reducing energy consumption and generating reactive species [11]. Granular activated carbon (GAC) is more widely used due to its high surface area, cost-effectiveness, and appropriate chemical stability [12]. In this study, aluminum electrodes were used due to their optimal consumption of electrical energy in the operating conditions [13], higher efficiency as an anode electrode compared with iron and zinc [14], lower cost than iron [15], and the acceptable efficiency in electrocoagulation process for the removal of CIP [16]. In addition to saving time and cost, designing an experiment provides optimum conditions for appropriate and reliable system performance. The response surface methodology (RSM) can take into account the interactions between variables and provide a mathematical model for predicting the process response. Additionally, some advantages are finding the optimal point outside of the tested points and presenting two and three-dimensional diagrams [17]. The experiment design and variable optimization affecting the process were performed using the central composite design (CCD). This study aimed to determine the efficiency of the three-dimensional electrochemical process with aluminum electrodes (3D-ECPWAE) for the removal of CIP from aqueous media and to improve the removal of CIP from synthetic aqueous solutions using a 3D-ECPWAE. The RSM coupled with CCD was used to evaluate the effects of different variables on the removal of CIP.

## 2. Experimental

### 2.1. Materials

The present study was conducted experimentally on a laboratory scale by a batch flow. CIP (>98%) (Table 1) was provided by Sigma Aldrich Co. Sulfuric acid (97%), sodium hydroxide (99%), sodium chloride (99%), and GAC were purchased from E. Merck. Hailea Air Pump (ACO-5503) with an aeration capacity of 3.5 $min^{-1}$. Plexiglas and aluminum sheets and the COD reactor (Aqualytic, Germany) were also used. CIP and COD readings were performed by HACH DR 5000 UV-Vis spectrophotometer and total organic carbon (TOC) meter (Vario TOC cube) made in Elementar Co.

### 2.2. Apparatus and procedure

Experiments were performed on 30 different runs, and four parameters were examined in each run. Therefore, overall, 120 different analyzes were performed.

A schematic of the 3D electrode reactor is shown in Fig. 1. A 3D reactor with a useful volume of 1,000 mL was made of plexiglass with internal dimensions (10.2 cm × 10 cm × 15 cm). The anode and cathode electrodes were made of the aluminum sheet with dimensions (10 cm × 10 cm × 0.04 cm) inside the reactor at a distance of 9 cm from each other. Sample volume 1,000 mL in each RUN, the amount of 10 g of cylindrical GAC (0.8–4 mm), was laid in the space between the electrodes as particle electrodes [7,18].

In order to prepare synthetic wastewater, a CIP stock solution at 500 mg/L concentration out of 0.5 g of CIP powder in 1,000 mL distilled water was used. Then, the pH of the solution was adjusted using $H_2SO_4$ and NaOH [19]. This solution was used to prepare more dilute samples to plot the standard curve and prepare a synthetic wastewater sample. In order to plot the standard curve, seven series of CIP solutions were prepared with different concentrations. After reading the adsorption values, the corresponding standard curve was plotted ($R^2 > 0.99$). Then, having set the values of the variables studied according to Table 2, the wastewater sample was injected into the reactor during various RUNs. The system started operating by connecting the electrodes to the DC power supply and aerating from the reactor. The sampling was performed at 30, 60, and 120 min at a depth of 5 cm during operation. The samples were filtered using Whatman-42 filter paper. The remaining CIP in the samples was read by a UV spectrophotometer at a $\lambda = 275$ nm [20,21]. Removal efficiency (RE%) of the CIP, COD, and TOC was calculated by measuring the concentration before and after the process, according to Eq. (1), where $C_i$ and $C_e$ are, respectively, initial and final concentrations (mg/L) of CIP, COD, and TOC [4]. After completing the experiments and optimizing the variables, COD measurement was performed using CRCM (closed reflux colorimetric method) according to the standard instruction No. 5220. D [22] and the residual TOC was measured by TOC meter (high-temperature combustion method instruction No. 5310. B) [19].

$$\text{RE}(\%) = \frac{(C_i - C_e)}{C_i} \times 100 \tag{1}$$

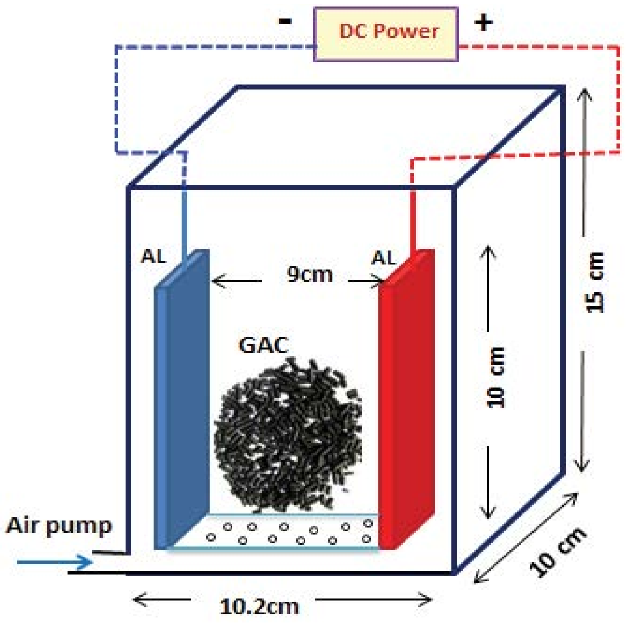

Fig. 1. Schematic of the 3D electrode reactor.

Table 1
General characteristics of ciprofloxacin

| | |
|---|---|
| Molecular formula | $C_{17}H_{18}FN_3O_3$ |
| Molecular weight | 331.346 g/mol |
| $\lambda_{max}$ | 275 nm |
| Chemical structure | 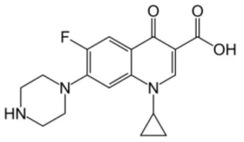 |

### 2.3. Fitting the model and process optimization

Major optimization phases include performing statistical experiments, estimating coefficients in a mathematical model, predicting the response, and examining the model adequacy [23]. Therefore, the model must be validated before use. For this purpose, model validation analyses can be used, including the independent data, normal data, constant variance between the levels, and the functional model's accuracy. The results indicate the internally studentized residuals vs. run number, the normality of the data, and residual values vs. predicted values. The validity of the model is analyzed by ANOVA. The results were analyzed to investigate the effects of variables, optimize the process and present the model.

### 2.4. Model selection

One of the steps in the analysis is to select the appropriate model for the system to predict the results with high accuracy. For this purpose, using the Best Subset Selection method, a quadratic model was used in Eq. (2), among all possible models. In this model, the five terms are related to linear effects (*A*, *B*, *C*, *D*, *E*), two terms are related to quadratic effects ($A^2$, $B^2$), while seven terms are assigned to interaction effects (*AB*, *AC*, *AE*, *BC*, *BD*, *CD*, *DE*), and Eff represents the predicted efficiency of the model for removal of CIP. Finally, the number of runs was 30, and in each run, 3 tests were performed, so the number of total tests was 90.

Table 2
Levels of variables studied in the removal of CIP

| Variables | Unit | Symbol | Levels studied | | | | |
|---|---|---|---|---|---|---|---|
| | | | +2 | +1 | 0 | –1 | –2 |
| pH | – | *A* | 10 | 8.5 | 7 | 5.5 | 4 |
| CIP concentration ($C_o$) | mg/L | *B* | 100 | 80 | 60 | 40 | 20 |
| Electrolyte concentration (NaCl) | g/L | *C* | 1 | 0.8 | 0.6 | 0.4 | 0.2 |
| Current intensity (*I*) | A | *D* | 1.5 | 1.25 | 1 | 0.75 | 0.5 |
| Operation time (*T*) | min | *E* | – | 120 | 60 | 30 | – |

$$\begin{aligned}\%\text{Eff} = {} & 83.44 - 2.184A + 3.391B - 0.88C + 1.655D \\ & + 0.814E - 1.634A^2 - 2.361B^2 - 0.022AB \\ & - 0.833AC + 0.663AE - 0.694BC + 0.646BD \\ & + 3.035CD + 0.666DE \end{aligned} \tag{2}$$

### 2.5. Model validation

#### 2.5.1. Investigating the normality of the residuals

The diagrams (a) and (b) are depicted in Fig. 2 to demonstrate this component. Diagram (a) is dedicated to the normal variables. It shows the normality of the data, given the linear points and their proximity to the reference line. According to the histogram of the residual or diagram (b), the bell-shaped pattern was observed.

#### 2.5.2. Investigating the variance function stability

Diagram (c) in Fig. 2 indicates the variance function stability of the model. This diagram shows the residual values vs. the fitted values. According to this diagram, the fit of the variance function stability of the residuals can be concluded.

#### 2.5.3. Investigating the error independence

Fig. 2d shows the error independence. In this diagram, the residual values vs. experiment order are plotted, and this random pattern indicates their independence.

#### 2.5.4. Investigating the model adequacy

According to the results (ANOVA) in Table 3, the "Lack-of-Fit" has a $P < 0.001$, which is significant. This statistical significance means the model is not accurate. However, the fitted values vs. the actual removal values were very close.

#### 2.5.5. Regression analysis

Regression indicators $R^2$, adjusted $R^2$ ($R^2$-adj), and predicted $R^2$ ($R^2$-pred) of the model were 0.76, 0.72, and 0.63, respectively. The $R^2$-pred of 0.63 was in reasonable agreement with the $R^2$-adj of 0.72 as their difference was

Table 3
Analysis of variance and uncertainty testing for removal of CIP

| Source | DF | Adj. SS | Adj. MS | *F*-value | *P*-value |
|---|---|---|---|---|---|
| Model | 14 | 2,672.74 | 190.910 | 16.93 | 0.000 |
| Linear | 5 | 1,456.07 | 291.214 | 25.83 | 0.000 |
| pH | 1 | 337.40 | 337.396 | 29.92 | 0.000 |
| $C_o$ | 1 | 827.91 | 827.906 | 73.43 | 0.000 |
| NaCl | 1 | 55.70 | 55.704 | 4.94 | 0.029 |
| *I* | 1 | 193.86 | 193.865 | 17.19 | 0.000 |
| Time | 1 | 41.20 | 41.199 | 3.65 | 0.060 |
| Square | 2 | 638.42 | 319.208 | 28.31 | 0.000 |
| pH × pH | 1 | 227.90 | 227.905 | 20.21 | 0.000 |
| $C_o \times C_o$ | 1 | 475.81 | 475.808 | 42.20 | 0.000 |
| 2-Way Interaction | 7 | 562.44 | 80.349 | 7.13 | 0.964 |
| pH × $C_o$ | 1 | 0.02 | 0.023 | 0.00 | 0.090 |
| pH × NaCl | 1 | 33.28 | 33.283 | 2.95 | 0.000 |
| pH × Time | 1 | 21.88 | 21.880 | 1.94 | 0.168 |
| $C_o$ × NaCl | 1 | 23.09 | 23.088 | 2.05 | 0.157 |
| $C_o$ × I | 1 | 20.03 | 20.034 | 1.78 | 0.187 |
| NaCl × *I* | 1 | 442.08 | 442.078 | 39.21 | 0.000 |
| *I* × Time | 1 | 22.06 | 22.057 | 1.96 | 0.166 |
| Error | 75 | 845.62 | 11.275 | | |
| Lack-of-fit | 60 | 831.77 | 13.863 | 15.02 | 0.000 |
| Pure error | 15 | 13.84 | 0.923 | | |
| Total | 89 | 3,518.35 | | | |

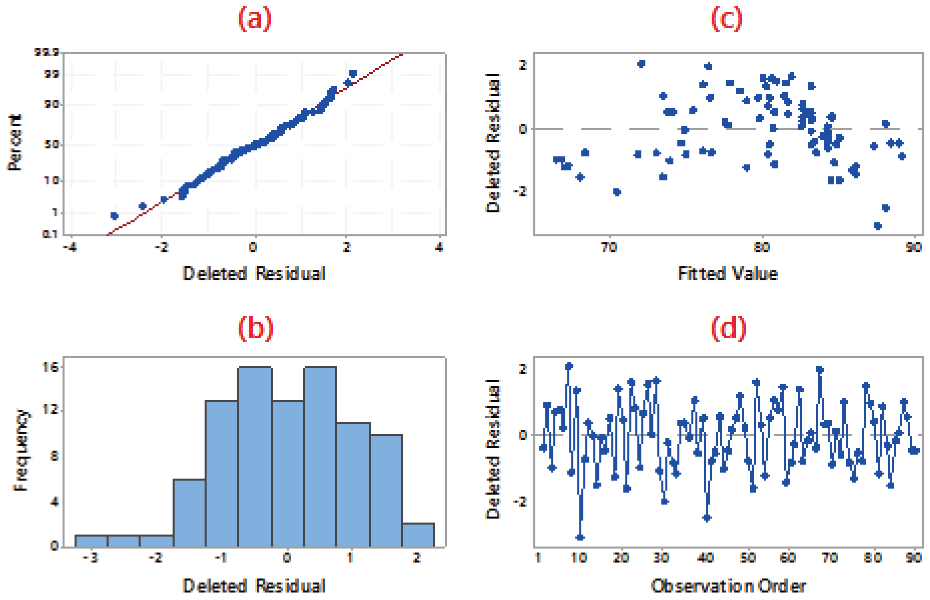

Fig. 2. Diagram (a) of normal variables, (b) histogram of residual particles, (c) residual values vs. fitted values, and (d) residual values vs. experiment order.

<0.2 [16,24]. Therefore, the appropriateness of the model is confirmed.

## 3. Results and discussion

### 3.1. Effect of pH

According to the ANOVA results (Table 3), the pH has a $P < 0.001$, $F$ (29.92), and it has quadratic effects. Therefore, pH is one of the most important factors affecting process efficiency. According to Fig. 3a, pH changes from 2 to 5.9 indicate that the CIP removal efficiency depends on the pH value. The maximum efficiency was reported at pH (5.92). Thereafter, the increased pH has reverse effects, and the process efficiency is reduced. CIP has different solubility and structure at different pHs. In acidic medium (pH < 6.1), the cationic form ($CH^+$) predominates due to the protonation of the amine group in the piperazine section. However, in the alkaline medium (pH > 8.7), the anionic ($CH^-$) form predominates because of the carboxylic group ionization. In the neutral medium (pH = 5.5–7.7), Zwitterion ($CH^\pm$) is dominant, which is obtained by the load balance between the two preceding groups [21,25,26]. Therefore, the chemical structure and the variability solubility of CIP cause efficiency changes in various processes such as adsorption and oxidation. Because of the insolubility of CIP at neutral pH, the max efficiency for CIP removal is obtained at pH (5.8). Out of this range, CIP is soluble, so removal efficiency is reduced [26]. In a study by Parsa et al. [16], the max removal efficiency of CIP by the electro-coagulation process was obtained at pH (5.6). In this study, the process efficiency reached the max value at pH (5.92). However, the increased pH resulted in a decrease in efficiency. Given the predictions made by the software in the optimization experiments and taking into account the operational factors, the optimal operating pH was (5.8). Although according to the solutions presented in Table 4, the optimal proposed pH was (5.92), which was consistent with the results of other studies.

### 3.2. Effect of initial CIP concentration ($C_o$)

According to Table 3, the relationship between initial concentration ($C_o$) and removal efficiency was significant. $C_o$ ($P < 0.001$). Thus, it is considered the most effective factor in process efficiency. According to Fig. 3b, the efficiency of CIP removal is gradually increased by increasing the $C_o$ from 20 mg/L to about 80 mg/L. Subsequently, an increase in the $C_o$ shows that the effect is reversed, and the

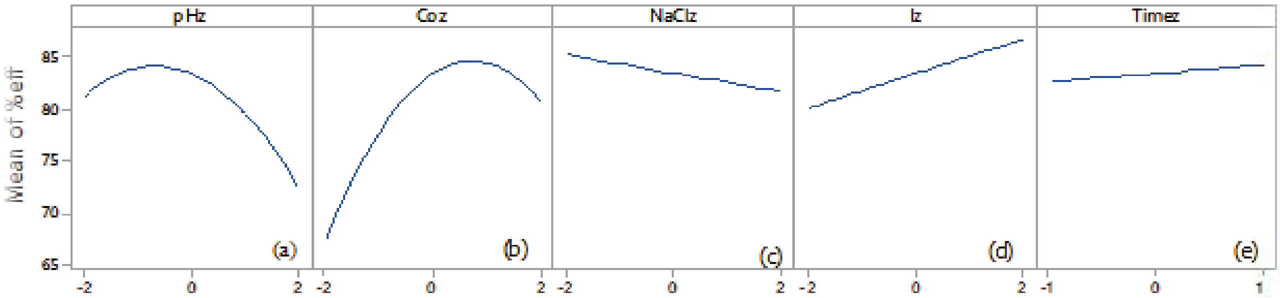

Fig. 3. The effect of the main variables within the encoded range.

Table 4
Experimental optimization, actual and fitted CIP efficiency level, COD and TOC removal effectiveness based on encoded levels

| Solution | pH | $C_o$ | NaCl | $I$ | $T$ | %Eff fit | %Eff actual | %Eff COD | %Eff TOC |
|---|---|---|---|---|---|---|---|---|---|
| 1 | –0.717 | 0.434 | 1 | 1 | 1 | 90.03 | | | |
| 2 | –0.855 | 0.052 | 1 | 1 | 1 | 89.65 | | | |
| 3 | $-7.45(10)^{-2}$ | 0.487 | 1 | 1 | 1 | 89.34 | | | |
| 4 | 0 | 0.425 | 1 | 1 | 1 | 89.18 | | | |
| 5 | 0.069 | 0.123 | 1 | 1 | 1 | 88.78 | | | |
| 6 | –0.802 | 1 | –1 | –1 | –1 | 88.5 | 86.72 | 48.04 | 45.45 |
| 7 | –1 | 0.561 | 0.56 | 1 | 0.48 | 88.30 | | | |
| 8 | –1 | 0.36 | 1 | 1 | –0.96 | 88.29 | | | |
| 9 | –0.572 | 1 | –1 | –1 | 0.98 | 88.09 | | | |
| 10 | –0.667 | 0.356 | 1 | 1 | –0.87 | 88.07 | | | |
| 11 | $-1.77(10)^{-2}$ | 0.997 | –1 | –1 | –0.96 | 87.96 | | | |
| 12 | 0.235 | 0.835 | –1 | –1 | 1 | 87.89 | | | |
| 13 | 0.292 | 0.998 | –1 | –1 | 1 | 87.87 | | | |
| 14 | 0.021 | 0.756 | –1 | –1 | –0.96 | 87.74 | | | |
| 15 | –0.375 | 0.34 | 1 | 1 | –0.89 | 87.48 | | | |

process efficiency is reduced. In similar studies, the efficiency decreased with increasing contaminant concentration, and the need for the electrical potential for the electrocoagulation process increased [27].

The increased $C_o$ increases the amount of organic compounds, resulting in an increase in the amount of competitive $OH^•$ consumption. Since the amount of $OH^•$ produced in the system is a certain amount, fewer organic compounds are degraded by $OH^•$. On the other hand, the formation of intermediate products during the degradation of organic compounds in the reaction reduces the access to $OH^•$ and reduces the removal efficiency of CIP. Özcan et al. [28] tried to remove CIP by photocatalytic process and showed that the removal efficiency was reduced by increasing the pollutant concentration. According to the ANOVA results, the $C_o$ was introduced as the most effective factor in the 3D-ECPWAE efficiency. The removal efficiency of CIP increased gradually with an increase in the $C_o$ from 20 to 80 mg/L. The effect of increased $C_o$ was negated, and gradually the process efficiency was reduced. This process showed the highest efficiency (86.72%) at a relatively $C_o$ (80) mg/L as optimal concentration. Therefore, (80 mg/L) was selected as the optimal operating concentration. A study by Jung et al. [25] showed that the third electrode accelerated the de-colorization and increased COD removal efficiency. Many complex processes such as adsorption, desorption, oxidation, catalyticization, and electrocoagulation occur because of a particle electrode in the 3D-ECPWAE (7, 8) that improves performance. In the processes involving ion transfers, the role of the electrolyte is undeniable [28].

### 3.3. Effect of electrolyte concentration (NaCl)

According to the ANOVA results in Table 3, NaCl with $P$ (0.029), $F$ (4.49), and the non-quadratic effects, it can be concluded that it is the least effective factor in the process efficiency. According to Fig. 3c, the effect of the NaCl is small, with a slight and inverse slope. Accordingly, by increasing the NaCl from 0.2 to 1 g/L, the CIP removal efficiency is reduced. The electrolyte should be carefully selected since it is determined based on a proper voltage, directly associated with energy consumption and operational costs [26]. Different NaCl may provide the required intensity, but in lower NaCl, higher voltages are needed to meet the desired intensity [18,26]. Since adding NaCl is less costly than applying a higher voltage and the wastewater is inherently sufficiently conductive, adding to the NaCl is less controversial than increasing the voltage [18,26]. The amount of electrolyte consumed should be able to provide the desired current intensity. Given the prediction in optimization experiments and different operational aspects in the max process efficiency, the optimal operating NaCl was 0.4 g/L. In a study by Chianeh et al. [16], the optimal operating NaCl for reactive dye removal by Ti/MWCNT electrode was obtained 1 g/L.

### 3.4. Effect of current intensity (I)

According to the study results in Table 3, current intensity affects the removal efficiency ($P < 0.001$). Thus, gradually increasing the $I$ to higher values increases the process efficiency. The effect of the current intensity is well known due to its important role in the electrochemical degradation of organic compounds since the amount of $OH^•$ depends mainly on the applied current [25]. In a study by Loukanov et al., the effect of the electrocoagulation method on the removal of colloidal contaminants was investigated. The results showed that with increasing current intensity from 2.5 to 10 mA/cm$^2$, the amount of pollutants deposited from 0.2 to 2 kg/m$^3$, which is consistent with the results of the present study. The 3D oxidation electrode radical follows an anodic mechanism; anodic oxidation is one of the most important electrochemical processes for the removal of resistant organic pollutants from water. In this process, strong oxidants such as $OH^•$ are produced according to reactions (3)–(5). According to the software prediction and the process efficiency, the $I$ (0.75) $A$ was selected as the optimal operating value.

$$H_2O \rightarrow H^+ + OH^• + e^- \tag{3}$$

$$O_2 + 2H^+ + 2e^- \rightarrow H_2O_2 \tag{4}$$

$$H_2O_2 + HO_2^• \rightarrow OH^• + O_2 + H_2O \tag{5}$$

### 3.5. Effect of operating time (T)

In this study, as the reaction time increased to the first 30 min, the removal efficiency increased, and the efficiency reached 86.72% (Fig. 3e). However, the efficiency did not increase significantly with an increase in $T$. Taking into account the other operational factors and solutions provided by the software, according to Table 4, a 30 min interval was selected as the optimal time. It can be said that the mineralization increases for some time, and then the removal rate progresses slowly. At first, the $OH^•$ is sufficient, but gradually the degradation of organic compounds reduces the efficiency of CIP removal. As time passes through, the formation of deposits on the electrodes decreases the CIP removal, or the process of degradation slows down once the sub-products resistant to electrochemical degradation are produced. The decrease in efficiency can also be attributed to the breakdown of CIP and the formation of simpler organic compounds [28].

### 3.6. Process optimization

The optimization software was used to obtain the highest efficiency of CIP removal, and the goal of maximizing response was determined. The lowest efficiency was 63.64% of the experimental observations, which was selected as the lower limit. However, the upper limit was 100% [14]. The software offers 15 solutions for the optimization experiments in order to obtain the max efficiency. The highest efficiency for the removal of CIP is given in Table 4 [24]. In this Tab, the first row shows the values for each variable with the highest efficiency at pH (5.92), $C_o$ (68/68) mg/L, NaCl (0.8) g/L, $I$ (1.5) $A$ and the operating time (120) min, and the max process efficiency for CIP removal was estimated 90.03%. It should be noted that the optimal conditions presented by the software has theoretical implications, and the software regards the highest efficiency as optimal. Therefore, the proposed solutions were evaluated in terms of operational and practical conditions. Finally, a solution was selected as the optimal operating conditions that was considerably more practical, required less time, less *I*, and low NaCl, and removed higher CIP. In these conditions, the pH (5.8), $C_o$ (80) mg/L, NaCl (0.4) g/L, *I* (0.75) *A*, *T* (30) min and the max efficiency was predicted 88.5%.

### 3.7. Confirmatory experiments

The optimal point was again investigated, and CIP removal efficiency in practice was compared with the estimated value of the model. The process efficiency for the removal of CIP was 86.72%. Therefore, the experimental removal efficiency (1.78) is erroneous compared to the predicted removal efficiency (Table 4), which is a slight error, indicating the validity of the fitted model.

### 3.8. Investigating the process efficiency for the removal of CIP, COD, and TOC in optimal operating conditions

COD and TOC values were measured to determine the process efficiency for the removal of COD and TOC, which play an important role in converting organic matter to minerals such as water and carbon dioxide in optimal condition (Table 4). According to Fig. 4, the CIP removal rate rises rapidly over the first 30 min once the process is started, reaching about 86.72%. As the operation time increases, the process continues with a very slight increase, and at 60 min, the efficiency reaches 87.66%. Thereafter, an increase in the operation time shows no positive effect on CIP removal rates. In this case, the efficiency of 86.72% is regarded as the optimal operational efficiency. In this case, 30 min is chosen as the optimal operation time [21]. According to Fig. 4, the COD removal rate rises rapidly and increases once the process is started and the operation time is increased up to 30 min. Hence, the removal rate reaches about 48.04%. From this time on, the effect of the operation time is reduced, but the increase in operation time still has a direct and positive effect on the removal efficiency of COD. This incremental process continues until 60 min after the start of the process. The max COD removal efficiency (60.78%) is seen at this phase. According to Fig. 4, the TOC removal rate increases rapidly once the process is started, and the operation time is increased up to 30 min, reaching 45.45%. Accordingly, 30 min after the reaction, the effect of time is reduced, but the increase in operation time still has a direct and positive effect on the removal efficiency of TOC. This increase is still observed for up to an hour. The max removal efficiency of TOC (56.57%) is achieved at this phase (21). The comparison of the removal efficiency of CIP, COD, and TOC by the 3D-ECPWAE in optimal conditions in Fig. 4 shows that the process efficiency in CIP removal is higher than COD and TOC [21].

## 4. Conclusion

According to this study, the removal efficiency of CIP, COD, and TOC increased rapidly 30 min after the start of the process and reached 86.72%, 48.04%, and 45.45%, respectively. This efficiency was achieved in optimum conditions, the pH (5.8), $C_o$ (80) mg/L, NaCl (0.4) g/L, *I* (0.75) *A*. Then, as the operating time goes up, the removal rate is slowed down. After 1 h, the removal efficiency reaches 87.06%, 60.78%, and 56.57%, respectively. In this study, the maximum efficiency of the three-dimensional electrochemical process with aluminum electrodes for CIP removal was obtained in optimal operating conditions (86.72%). Although, the maximum efficiency was estimated at 90.03% at pH (5.92), $C_o$ (68/68) mg/L, NaCl (0.8) g/L, *I* (1.5) *A* and *T* (120) min. However, after an hour of the operation time, the improvement in COD and TOC removal efficiency is more than the CIP removal efficiency (87.04%, 60.78%, and 56.57%), which means that the mineralization of organic compounds caused by the degradation of CIP is an appropriate process 1 h after the reaction is completed. Finally, the results showed that 3D-ECPWAE has an acceptable efficiency for removal of CIP, COD, and TOC, and RSM

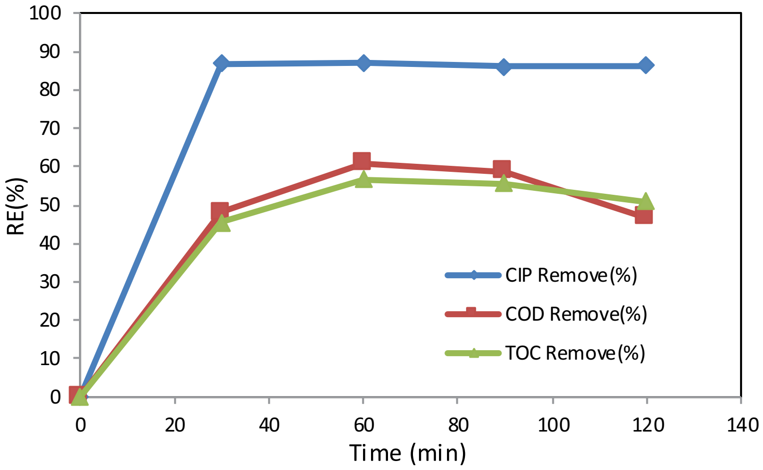

Fig. 4. The process efficiency in removing CIP, COD, and TOC in optimal condition vs. time of the process.

is an efficient method for optimizing the operational conditions and predicting the efficiency of CIP removal by this process.

## Acknowledgments

This work was supported by the Vice Chancellorship for Research Affairs of UMSHA (No. 9609075614). We are grateful to Hamadan University of Medical Sciences for providing research materials, equipment, and funds. The authors declare that they have no conflicts of interest.

## References

[1] N. Dhiman, N. Sharma, Removal of ciprofloxacin hydrochloride from aqueous solution using vertical bed and sequential bed columns, J. Environ. Chem. Eng., 6 (2018) 4391–4398.

[2] S. Majidi, A. Rahmani, M. Samadi, R. Shokoohi, Determination of sono-electrofenton efficiency in removal of ciprofloxacin antibiotic from aqueous solutions, Sci. J. Ilam Univ. Med. Sci., 23 (2016) 85–96.

[3] H. Liu, W. Liu, J. Zhang, C. Zhang, L. Ren, Y. Li, Removal of cephalexin from aqueous solutions by original and Cu(II)/Fe(III) impregnated activated carbons developed from lotus stalks: kinetics and equilibrium studies, J. Hazard. Mater., 185 (2011) 1528–1535.

[4] W. Duan, N. Wang, W. Xiao, Y. Zhao, Y. Zheng, Ciprofloxacin adsorption onto different micro-structured tourmaline, halloysite and biotite, J. Mol. Liq., 269 (2018) 874–881.

[5] X. Du, Y. Zhang, I. Hussain, S. Huang, W. Huang, Insight into reactive oxygen species in persulfate activation with copper oxide: activated persulfate and trace radicals, Chem. Eng. J., 313 (2017) 1023–1032.

[6] P.V. Nidheesh, R. Gandhimathi, Trends in electro-Fenton process for water and wastewater treatment: an overview, Desalination, 299 (2012) 1–15.

[7] S. Sowmiya, R. Gandhimathi, S.T. Ramesh, P.V. Nidheesh, Granular activated carbon as a particle electrode in three-dimensional electrochemical treatment of reactive black B from aqueous solution, Environ. Prog. Sustainable Energy, 35 (2016) 1616–1622.

[8] C. Zhang, Y. Jiang, Y. Li, Z. Hu, L. Zhou, M. Zhou, Three-dimensional electrochemical process for wastewater treatment: a general review, Chem. Eng. J., 228 (2013) 455–467.

[9] H. Pourzamani, N. Mengelizadeh, H. Mohammadi, N. Niknam, B. Neamati, R. Rahimi, Comparison of electrochemical advanced oxidation processes for removal of ciprofloxacin from aqueous solutions, Desal. Water Treat., 113 (2018) 307–318.

[10] H. Pourzamani, Y. Hajizadeh, N. Mengelizadeh, Application of three-dimensional electro-Fenton process using MWCNTs-$Fe_3O_4$ nanocomposite for removal of diclofenac, Process Saf. Environ. Prot., 119 (2018) 271–284.

[11] H. Mohammadi, A. Alinejad, M. Khajeh, M. Darvishmotevalli, M. Moradnia, A.M. Tehrani, G. Hosseindost, M.R. Zare, N. Mengelizadeh, Optimization of the 3D electro-Fenton process in removal of acid orange 10 from aqueous solutions by response surface methodology, J. Chem. Technol. Biotechnol., 94 (2019) 114–125.

[12] R. Mao, X. Zhao, H. Lan, H. Liu, J. Qu, Graphene-modified Pd/C cathode and Pd/GAC particles for enhanced electrocatalytic removal of bromate in a continuous three-dimensional electrochemical reactor, Water Res., 77 (2015) 1–12.

[13] S. Ahmadzadeh, A. Asadipour, M. Pournamdari, B. Behnam, H.R. Rahimi, M. Dolatabadi, Removal of ciprofloxacin from hospital wastewater using electrocoagulation technique by aluminum electrode: optimization and modelling through response surface methodology, Process Saf. Environ. Prot., 109 (2017) 538–547.

[14] R. Kamaraj, D.J. Davidson, G. Sozhan, S. Vasudevan, Adsorption of herbicide 2-(2,4-dichlorophenoxy)propanoic acid by electrochemically generated aluminum hydroxides: an alternative to chemical dosing, RSC Adv., 5 (2015) 39799–39809.

[15] Z. Beril Gönder, G. Balcıoğlu, I. Vergili, Y. Kaya, Electrochemical treatment of carwash wastewater using Fe and Al electrode: techno-economic analysis and sludge characterization, J. Environ. Manage., 200 (2017) 380–390.

[16] J.B. Parsa, T.M. Panah, F.N. Chianeh, Removal of ciprofloxacin from aqueous solution by a continuous flow electro-coagulation process, Korean J. Chem. Eng., 33 (2016) 893–901.

[17] A.R. Rahmani, H. Almasi, S. Bajalan, H. Rezaei Vahidian, A. Zarei, A. Shabanloo, Optimization of ciprofloxacin antibiotic sonochemical degradation with persulfate activated by nano zero-valent iron by central composite design method, J. Health, 8 (2017) 231–245.

[18] W. Can, H. Yao-Kun, Z. Qing, J. Min, Treatment of secondary effluent using a three-dimensional electrode system: COD removal, biotoxicity assessment, and disinfection effects, Chem. Eng. J., 243 (2014) 1–6.

[19] M.T. Samadi, R. Shokohi, R. Harati, Comparison of heterogeneous Fenton process and adsorption process on magnetic nanocomposite for ciprofloxacin removal from aqueous solutions, J. Inflammatory Dis., J. Qazvin Univ. Med. Sci., 20 (2016) 4–13.

[20] J.W. Peterson, L.J. Petrasky, M.D. Seymour, R.S. Burkhart, A.B. Schuiling, Adsorption and breakdown of penicillin antibiotic in the presence of titanium oxide nanoparticles in water, Chemosphere, 87 (2012) 911–917.

[21] F.R. Espinoza-Quiñones, A.R.C. de Souza, A.N. Módenes, D.E. Trigueros, A.R. de Pauli, P.S.C. de Souza, A.D. Kroumov, Removal performance, antibacterial effects, and toxicity assessment of ciprofloxacin treated by the electrocoagulation process, Water Air Soil Pollut., 227 (2016) 460, doi: 10.1007/s11270-016-3165-8.

[22] APHA, AWWA, WEF, Standard Methods for the Examination of Water and Wastewater, National Government Publication, 21st ed., American Public Health Association (APHA), American Water Works Association (AWWA), Water Environment Federation (WEF), Washington, D.C., 2005.

[23] S. Sugashini, K.M. Meera Sheriffa Begum, Optimization using central composite design (CCD) for the biosorption of Cr(VI) ions by cross linked chitosan carbonized rice husk (CCACR), Clean Technol. Environ. Policy, 15 (2013) 293–302.

[24] Barışçı S, Turkay O. Optimization and modelling using the response surface methodology (RSM) for ciprofloxacin removal by electrocoagulation. Water Science and Technology. 2016;73(7):1673–9.

[25] K.-W. Jung, M.-J. Hwang, D.-S. Park, K.-H. Ahn, Combining fluidized metal-impregnated granular activated carbon in three-dimensional electrocoagulation system: feasibility and optimization test of color and COD removal from real cotton textile wastewater, Sep. Purif. Technol., 146 (2015) 154–167.

[26] M. Foroughi, H.R.S. Arezoomand, A.R. Rahmani, G. Asgari, D. Nematollahi, K. Yetilmezsoy, M.R. Samarghandi, Electrodegradation of tetracycline using stainless steel net electrodes: screening of main effective parameters and interactions by means of a two-level factorial design, Korean J. Chem. Eng., 34 (2017) 2999–3008.

[27] E. Bazrafshan, A.H. Mahvi, S. Nasseri, M. Shaieghi, Performance evaluation of electrocoagulation process for diazinon removal from aqueous environments by using iron electrodes, Iran. J. Environ. Health Sci. Eng., 4 (2007) 127–132.

[28] A. Özcan, Y. Şahin, A. Savaş Koparal, M.A. Oturan, A comparative study on the efficiency of electro-Fenton process in the removal of propham from water, Appl. Catal., B, 89 (2009) 620–626.